Effect of system energy on quantum signatures of chaos in the two-photon Dicke model

Shangyun Wang,[1,*] Songbai Chen,[1,2,†] and Jiliang Jing[1,2,‡]

[1]*Department of Physics, Key Laboratory of Low Dimensional Quantum Structures and Quantum Control of Ministry of Education, and Synergetic Innovation Center for Quantum Effects and Applications, Hunan Normal University, Changsha, Hunan 410081, People's Republic of China*

[2]*Center for Gravitation and Cosmology, College of Physical Science and Technology, Yangzhou University, Yangzhou 225009, People's Republic of China*

(Received 16 February 2019; revised manuscript received 10 July 2019; published 12 August 2019)

We have studied entanglement entropy and Husimi Q distribution as a tool to explore chaos in the quantum two-photon Dicke model. With the increase of the energy of a system, the linear entanglement entropy of a coherent state prepared in the classical chaotic and regular regions becomes more distinguishable, and the corresponding relationship between the distribution of time-averaged entanglement entropy and the classical Poincaré section has clearly been improved. Moreover, Husimi Q distribution for the initial states corresponding to the points in the chaotic region in the higher-energy system disperses more quickly than that in the lower-energy system. Our results imply that higher system energy has contributed to distinguishing between the chaotic and regular behavior in the quantum two-photon Dicke model.

DOI: 10.1103/PhysRevE.100.022207

I. INTRODUCTION

It is well known that classical chaos is a complex motion with a high sensitivity to initial conditions. It appears in nonlinearly dynamical systems and can usually be detected by such methods as Poincaré surfaces of section and Lyapunov characteristic exponents. However, the chaos in quantum mechanics has become more intriguing and challenging because there is no general quantum counterpart of classical phase-space trajectories due to the uncertainty principle [1–4]. Moreover, the scalar product between two nearby states with different initial conditions remains a constant for all time rather than an exponential divergence because of the unitary time-evolution operator. Therefore, it is very important to explore and explain the signatures of chaos in a quantum system, as it could help us to understand further the quantum dynamics itself and the correspondence principle between classical and quantum mechanics.

With the random matrix theory, Wigner *et al.* [5,6] analyzed statistical properties at different energy levels in a quantum chaos state, and they found that the distribution of spacings between adjacent energy levels for quantum chaos states obeys Wigner distributions governed by the Gaussian ensemble of matrices rather than the usual Poisson distribution. Moreover, the study of entanglement entropy indicates that, in general, chaotic systems tend to have larger entanglement entropy than regular systems [7–11]. However, the corresponding relationship between entanglement entropy and chaos does not always hold because there are certain cases in which the entanglement entropy for the initial state prepared in the regular region is higher than that in the chaotic region [12–14]. The intrinsic physics is still uncertain and needs to be investigated further. Recently, Ruebeck *et al.* [14] studied the entangling quantum kicked top and divided the infinite-time-averaged entanglement entropy S_Q into two parts, I_Q and R_Q, which come, respectively, from the "diagonal" and "off-diagonal" matrix elements of the angular momentum operators obtained by the Floquet eigenstates of the system. They found that I_Q and S_Q were correlated with a quantity I_c that is not equivalent to classical chaos. In the quantum kicked top model, Piga *et al.* [15] also found that by increasing the number of qubits, the entanglement entropy of the initial states in the classical regular and chaotic regions becomes more distinguishable, which leads to a clearer correspondence between the entanglement entropy and the classical features of the phase space. Moreover, they also found that there are certain similar behaviors between low entanglement entropy tori and Kolmogorov-Arnol'd-Noser (KAM) tori, which implies that entanglement could play an important role in quantum KAM theory. Efforts have been devoted to developing a quantum analog of KAM theory in Refs. [16–19]. Other quantum sources, such as spin squeezing [20], quantum discord [21], and an out-of-time ordered correlator [22–24], have been applied as signatures to explore chaos in quantum systems.

In this paper, we will focus on the two-photon Dicke model in which N identical two-level atoms couple to a bosonic mode through two-photon interaction. Such a two-photon interaction has been commonly applied to describe the second-order process in physical devices including quantum dots [25,26], trapped ions, and Rydberg atoms in microwave superconducting cavities [27,28]. Compared with the standard Dicke model [29], the presence of two-photon interaction results in some new properties appearing in this quantum system. For example, the discrete system spectrum collapses into

*shangyunwang@163.com

†Author to whom all correspondence should be addressed: csb3752@hunnu.edu.cn

‡jljing@hunnu.edu.cn

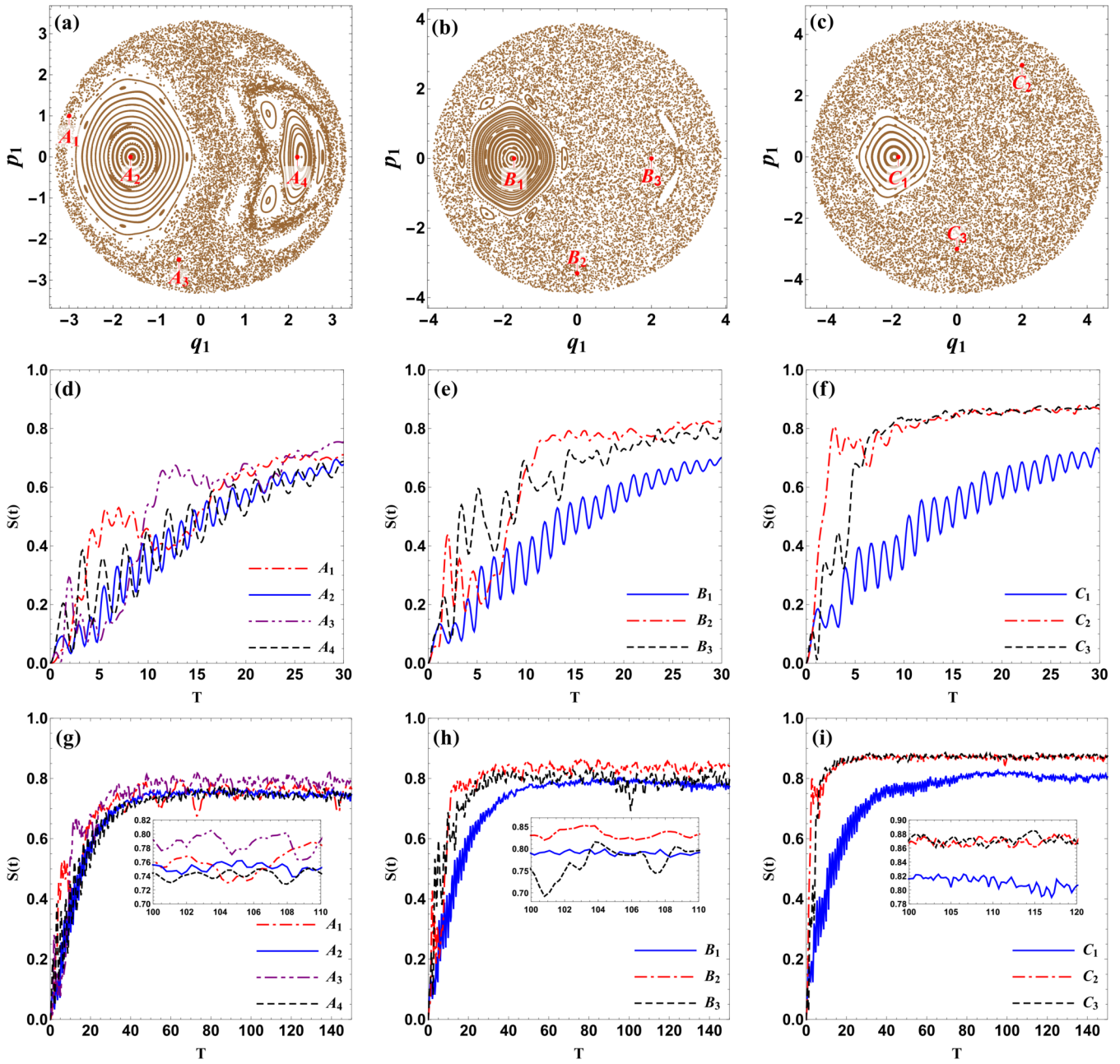

FIG. 1. Parts (a)–(c) correspond to the classical phase spaces for the two-photon Dicke model with system energy $E = 1$, 5, and 10, respectively. Points A_1, A_3, B_2, B_3, C_2, and C_3 are in classical chaotic regions, but points A_2, A_4, B_1, and C_1 are in classical regular regions. Parts (d)–(i) present the evolution of linear entanglement entropy $S(t)$ with time t for these points, respectively. A comparison of (d)–(f) or (h),(i) shows that as one increases the energy of the system, the linear entanglement entropies of the points between these chaotic and regular regions become more distinguishable. Here, we set $\omega = \omega_0/2 = 1$, $j = 5$, and $g = 0.3$.

a continuous band for a specific value of the coupling strength [30–32]. In the transition from the strong to the ultrastrong coupling regime, a continuous symmetry breaks down into a fourfold discrete symmetry described by a generalized-parity operator [33]. Moreover, a superradiant phase transition [34] also occurs in the two-photon Dicke model due to coherent radiation of the atoms. The behavior of finite-size scaling functions [35] in the two-photon Dicke model indicates that the superradiant phase transition has the same scaling features as in the standard Dicke model. Since two-photon coupling is a nonlinear interaction, the chaos phenomenon would appear in such dynamical systems. However, quantum signatures of chaos and the correspondence between entanglement and classical chaos are still open in the two-photon Dicke model. Moreover, in addition to increasing the particle number N as in the quantum kicked top model, there may be other ways to improve the correspondence between chaos and entanglement entropy. This is very interesting and it should be investigated further in a quantum system. The main motivation in this paper is to study entanglement entropy and Husimi Q distribution and to probe further the relationship between entanglement and classical chaos. We find that with higher

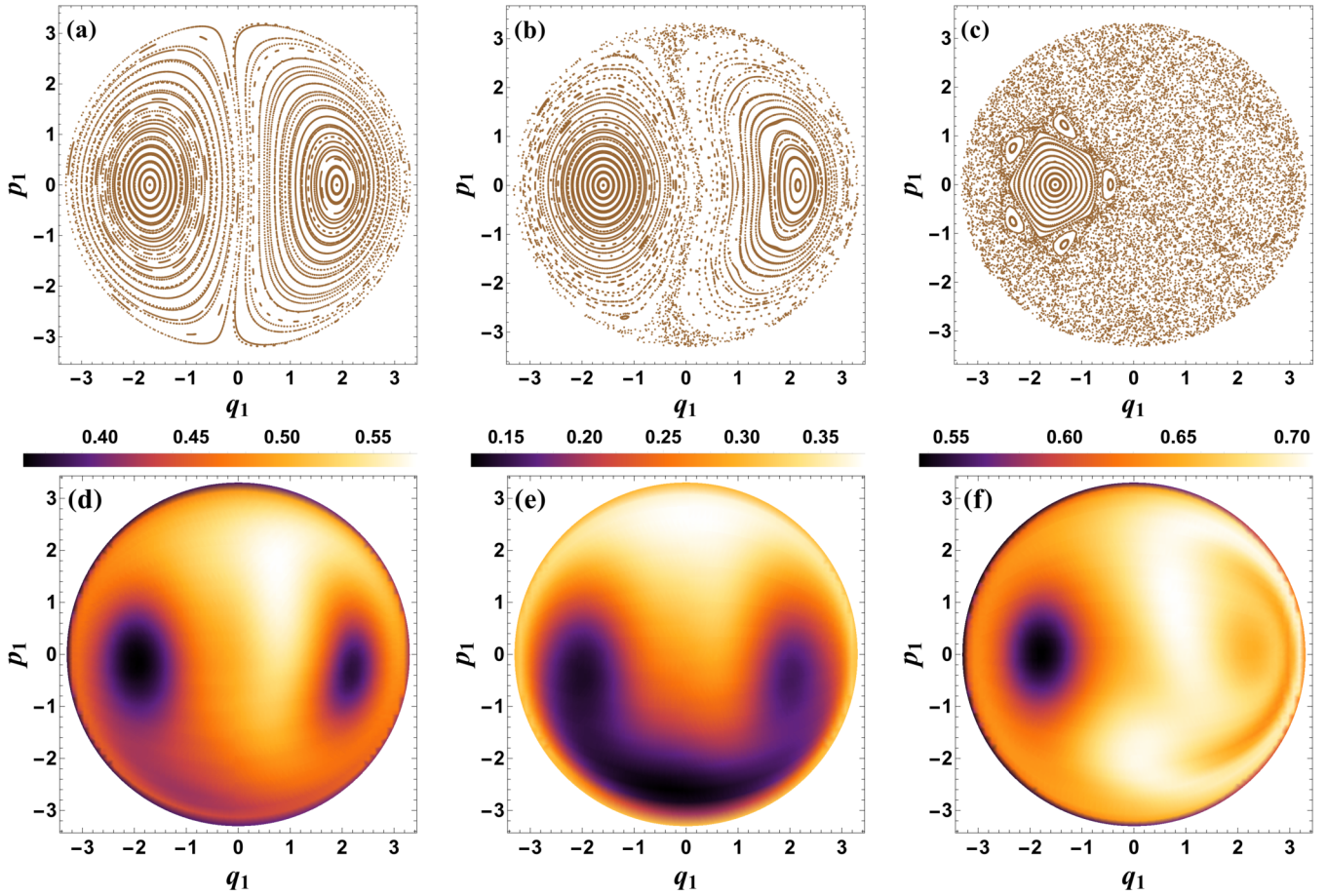

FIG. 2. Parts (a)–(c) correspond to the classical phase spaces for the two-photon Dicke model with the coupling parameter $g = 0.1$, 0.25, and 0.4, respectively. Parts (d)–(f) denote the corresponding time-averaged entanglement entropy distribution for the two-photon Dicke model with the coupling parameter $g = 0.1$, 0.25, and 0.4, respectively. Here, we set $\omega = \omega_0/2 = 1$, $j = 5$, and $E = 1$.

system energy, the values of linear entanglement entropy of the points between chaotic and regular regions become more distinguishable for the two-photon Dicke model. Meanwhile, the higher system energy clearly improves the corresponding relationship between the distribution of time-averaged entanglement entropy and the classical Poincaré section in this model.

The paper is organized as follows. In Sec. II, we introduces briefly the two-photon Dicke model and its properties. In Sec. III, we study the effects of system energy on the correspondence between the distribution of time-averaged entanglement entropy and the classical Poincaré section in the two-photon Dicke model. In Sec. IV, we analyze the Husimi Q distribution and further probe the effects of system energy on quantum signatures of chaos in this model. Finally, we present results and a brief summary.

II. THE TWO-PHOTON DICKE MODEL

Let us now briefly introduce the two-photon Dicke model in which N two-level identical atoms interact with a single bosonic mode through a two-photon interaction. The system Hamiltonian can be expressed as [29]

$$\hat{H} = \omega\hat{a}^\dagger\hat{a} + \omega_0\hat{J}_z + \frac{g}{N}(\hat{J}_+ + \hat{J}_-)(\hat{a}^2 + \hat{a}^{\dagger 2}), \qquad (1)$$

where $\hat{a}$ and $\hat{a}^\dagger$, respectively, are the annihilation and creation operators of the single-mode cavity with frequency ω. Here, ω_0 is the atomic transition frequency and g is the collective coupling strength of the two-photon interaction. $\hat{J}_z = \sum_{n=1}^{N}\hat{\sigma}_z^{(i)}/2$ is the two-level atomic inversion operator, and $\hat{J}_+ = \sum_{n=1}^{N}\hat{\sigma}_+^{(i)}/2$ and $\hat{J}_- = \sum_{n=1}^{N}\hat{\sigma}_-^{(i)}/2$ are the collective atomic raising and lowing operators. The operators $\hat{J}_z$, $\hat{J}_+$, and $\hat{J}_-$ form the SU(2) Lie algebra, which obeys the commutation relations

$$[\hat{J}_+, \hat{J}_-] = 2\hat{J}_z, \quad [\hat{J}_z, \hat{J}_\pm] = \pm\hat{J}_\pm. \qquad (2)$$

Compared with the usual standard Dicke model, the Hamiltonian in the two-photon Dicke model has a generalized Z_4 parity operator $\prod = (-1)^N \otimes_{n=1}^{N}\hat{\sigma}_z^n e^{i\pi\hat{a}^\dagger\hat{a}/2}$ with four eigenvalues (i.e., ± 1 and $\pm i$) rather than the Z_2 parity in the standard Dicke model [36,37].

To study the relationship between entanglement and classical chaos in the two-photon Dicke model, we take the initial states to be coherent states since they correspond to the minimum uncertainty wave packets centered in the classical phase space. As in Refs. [8,36–38], we choose the initial quantum states as

$$|\psi(0)\rangle = |\tau\rangle \otimes |\beta\rangle \equiv |\tau\beta\rangle, \qquad (3)$$

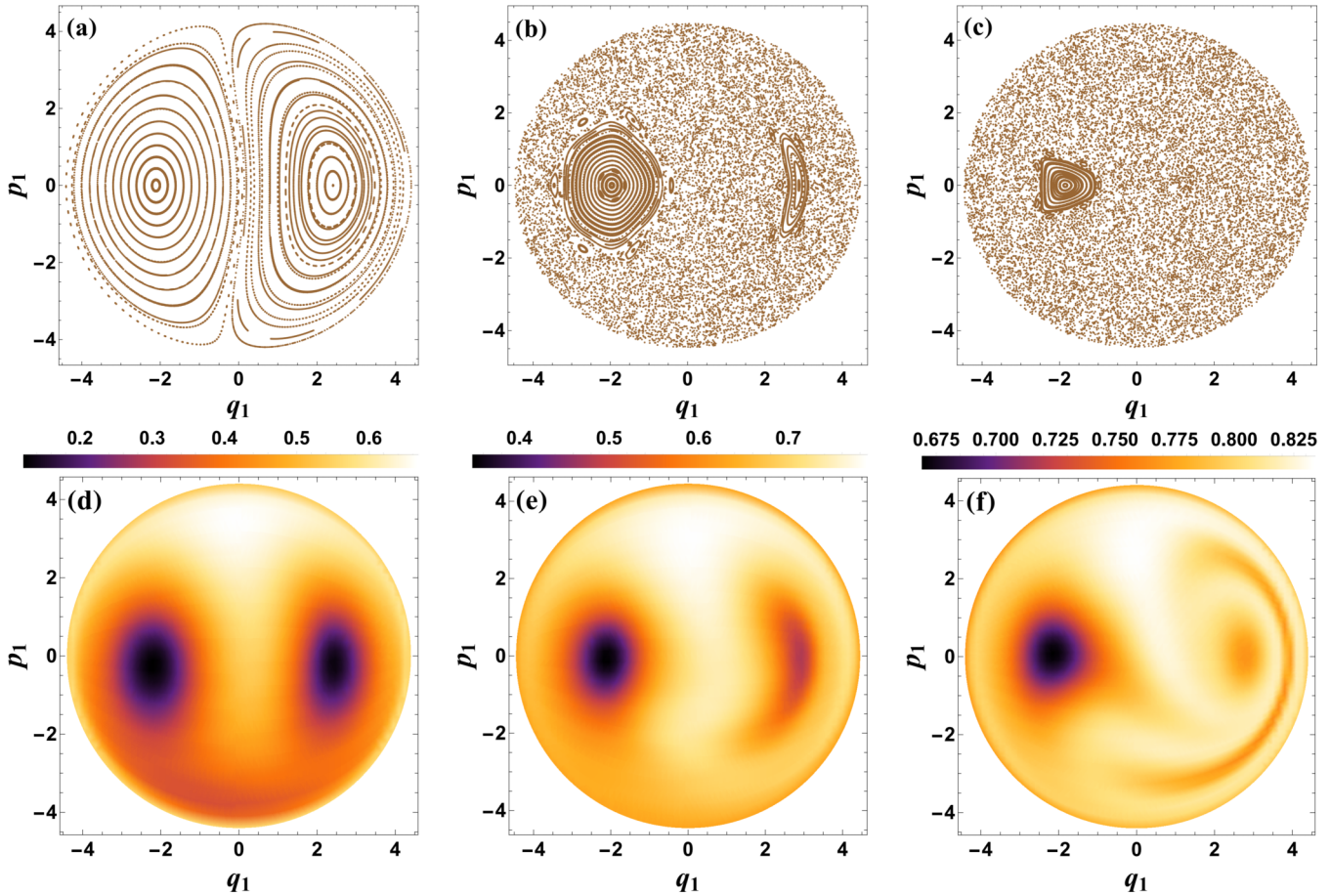

FIG. 3. Parts (a)–(c) correspond to the classical phase spaces for the two-photon Dicke model with the coupling parameter $g = 0.1$, 0.25, and 0.4, respectively. Parts (d)–(f) denote the corresponding time-averaged entanglement entropy distribution for the two-photon Dicke model with the coupling parameter $g = 0.1$, 0.25, and 0.4, respectively. Here, we set $\omega = \omega_0/2 = 1$, $j = 5$, and $E = 10$.

where $|\tau\rangle$ and $|\beta\rangle$ are the atomic and bosonic coherent states, respectively. The coherent states $|\tau\rangle$ and $|\beta\rangle$ have the forms

$$|\tau\rangle = (1 - \tau\tau^*)^{-j} e^{\tau \hat{J}_+} |J, -J\rangle,$$
$$|\beta\rangle = e^{-\beta\beta^*/2} e^{\beta \hat{a}^\dagger} |0\rangle, \tag{4}$$

with

$$\tau = \frac{q_1 + ip_1}{\sqrt{4j - q_1^2 - p_1^2}}, \quad \beta = \frac{1}{\sqrt{2}}(q_2 + ip_2). \tag{5}$$

Here $|J, -J\rangle$ denotes the state with spin J and $\hat{J}_z = -J$, and $|0\rangle$ is the bosonic field ground state. The quantity j is set to $j = N/2$ and the variables q_1, p_1, q_2, p_2 describe the phase space of the system. The indices 1 and 2 denote the atomic and field subsystems, respectively. With the standard procedure [38], one can obtain the corresponding classical Hamiltonian for the two-photon Dicke model (1),

$$H_{\rm cl} \equiv \langle \tau\beta|\hat{H}|\tau\beta\rangle = \frac{\omega_0}{2}\left(q_1^2 + p_1^2 - 2j\right) + \frac{\omega}{2}\left(q_2^2 + p_2^2\right) + \frac{q_1\sqrt{4j - q_1^2 - p_1^2}\left(q_2^2 - p_2^2\right)g}{2j}. \tag{6}$$

It is then easy to obtain Hamilton's canonical equations,

$$\dot{q}_1 = \omega_0 p_1 + \frac{g q_1 p_1 \left(p_2^2 - q_2^2\right)}{2j\sqrt{4j - q_1^2 - p_1^2}},$$
$$\dot{q}_2 = \omega p_2 - \frac{g q_1 p_2 \sqrt{4j - q_1^2 - p_1^2}}{j},$$
$$\dot{p}_1 = -\omega_0 q_1 + \frac{g\left(4j - 2q_1^2 - p_1^2\right)\left(p_2^2 - q_2^2\right)}{2j\sqrt{4j - q_1^2 - p_1^2}},$$
$$\dot{p}_2 = -\omega q_2 - \frac{g q_1 \sqrt{4j - q_1^2 - p_1^2}}{j}. \tag{7}$$

For the two-photon Dicke model, there is a spectral collapse at $g_{\rm collapse} = \frac{\omega}{2}$, which yields that the energy levels of the system collapse into a continuum as $g \geqslant \frac{\omega}{2}$ and then the ground state of Hamiltonian (1) is no longer defined in this regime. Therefore, we will focus on the strong-coupling regime, where g is smaller than but comparable to $\omega/2$. For the sake of simplicity, we limit our consideration to the resonant case $\omega_0 = 2\omega$ in which the transition between two energy levels occurs only if the atom absorbs (or emits) two photons. The presence of the two-photon interaction yields that the equation of motion

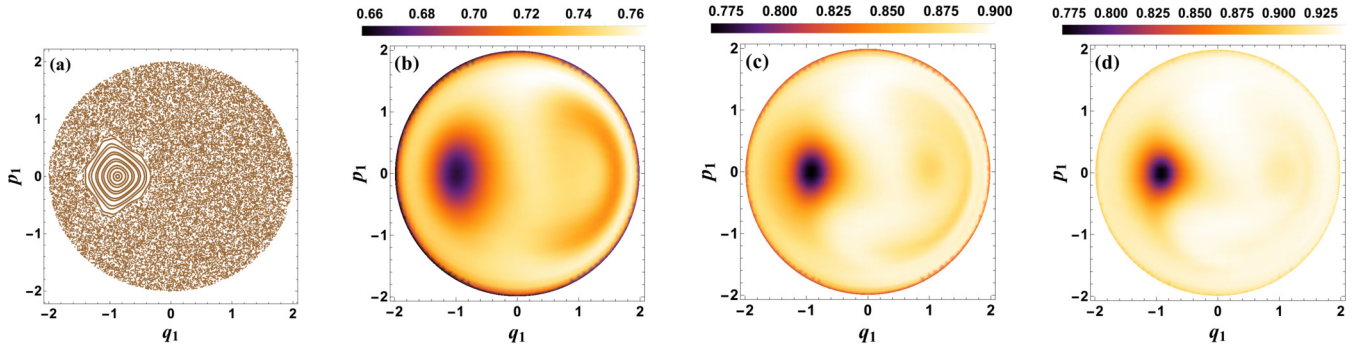

FIG. 4. The correspondence between classical dynamics and quantum entanglement entropy for the two-photon Dicke model with the fixed ratio $E/N = 1.1$. Part (a) is the classical Poincaré section, and (b)–(d) denote the corresponding time-averaged entanglement entropy distribution for the two-photon Dicke model with $E = 5.5, N = 5$; $E = 16.5, N = 15$; and $E = 33, N = 30$, respectively. Here we rescale $q1 \to q1/\sqrt{j}$, $p1 \to p1/\sqrt{j}$, and we set the coupling parameter $g = 0.3$ and $\omega = \omega_0/2 = 1$.

(7) in the classical correspondence is not variable-separable, which means that the corresponding motion could be chaotic. In Figs. 1(a)–1(c), we present the Poincaré section for certain parameters and initial values, which show that there is chaos for the system described by the classical Hamiltonian (6) corresponding to the two-photon Dicke model (1).

III. EFFECTS OF ENERGY OF A SYSTEM ON THE QUANTUM SIGNATURES OF CHAOS IN THE TWO-PHOTON DICKE MODEL

In this section, we will investigate how the system energy improves the quantum signatures of chaos in the two-photon Dicke model via linear entanglement entropy, which is a

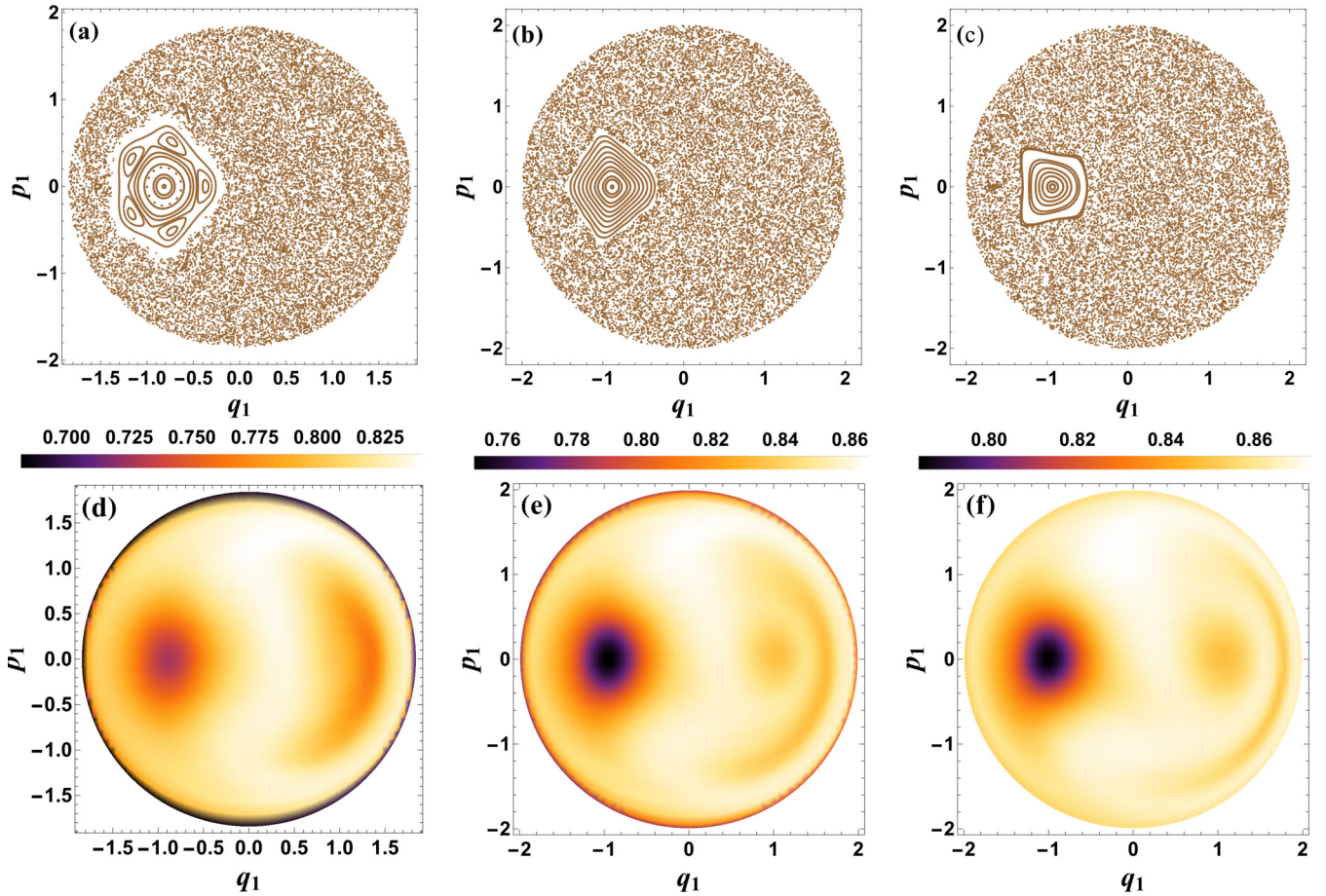

FIG. 5. The correspondence between classical dynamics and quantum entanglement entropy for the two-photon Dicke model with fixed particle number $N = 10$ and coupling constant $g = 0.3$. Parts (a)–(c) correspond to the classical phase spaces for the two-photon Dicke model with system energy $E = 7$, 12, and 17, respectively. Parts (d)–(f) denote the time-averaged entanglement entropy for the two-photon Dicke model with system energy $E = 7$, 12, and 17, respectively. Here we set $\omega = \omega_0/2 = 1$.

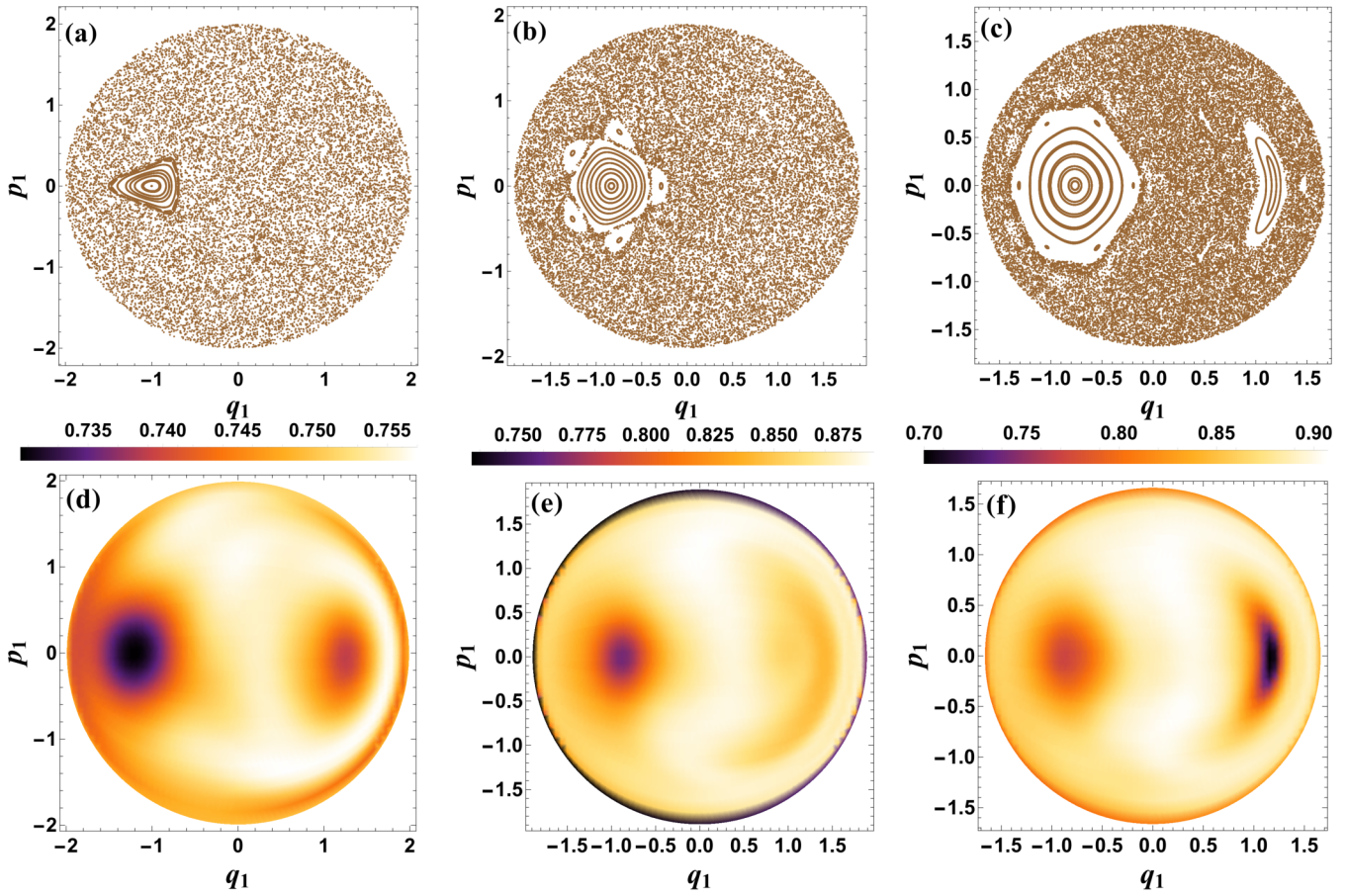

FIG. 6. The correspondence between classical dynamics and quantum entanglement entropy for the two-photon Dicke model with fixed system energy $E = 12$ and coupling constant $g = 0.3$. Parts (a)–(c) correspond to the classical phase spaces for the two-photon Dicke model with particle number $N = 4$, 15, and 30, respectively. Parts (d)–(f) denotes time-averaged entanglement entropy for the two-photon Dicke model with particle number $N = 4$, 15, and 30, respectively. Here we set $\omega = \omega_0/2 = 1$.

common tool to explore chaos in quantum systems including the Dicke model [8] and the kicked top model [11]. The linear entanglement entropy is defined as

$$S(t) = 1 - \mathrm{Tr}_1 \rho_1(t)^2, \tag{8}$$

with the reduced-density matrix

$$\rho_1(t) = \mathrm{Tr}_2 |\psi(t)\rangle\langle\psi(t)|, \tag{9}$$

where Tr_i is a trace over the ith subsystem ($i = 1, 2$), and the vector $|\psi(t)\rangle$ is the quantum state of the full system that evolved in time under the action of Hamiltonian (1). The quantity $S(t)$ describes the degree of purity of the subsystems and the degree of decoherence. In Figs. 1(d)–1(i), we show the evolution of linear entanglement entropy with time t for the different initial states, which correspond to different points in

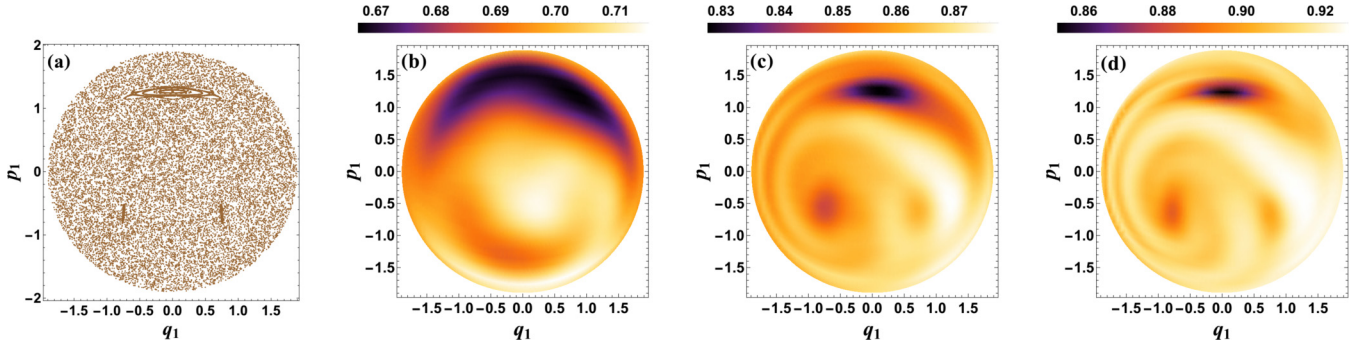

FIG. 7. The correspondence between classical dynamics and quantum entanglement entropy for the one-photon Dicke model with the fixed ratio $E/N = 0.4$. Part (a) is the classical Poincaré section, and (b)–(d) denote the time-averaged entanglement entropy for the one-photon Dicke model in the cases with $E = 2, N = 5$; $E = 6, N = 15$; and $E = 12, N = 30$, respectively. Here we rescale $q1 \to q1/\sqrt{j}$, $p1 \to p1/\sqrt{j}$, and we set the coupling parameter $g = 0.5$ and $\omega = \omega_0 = 1$.

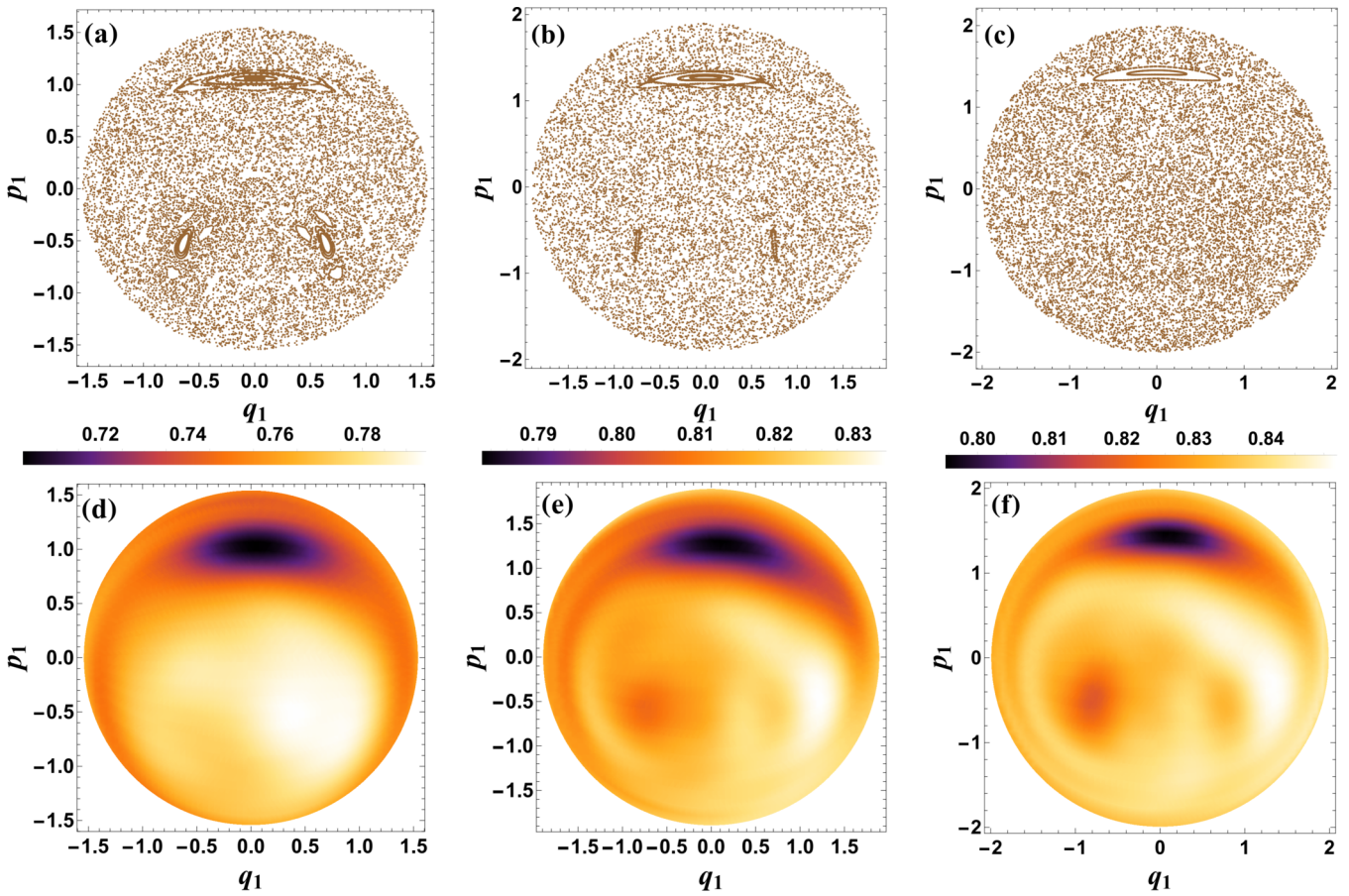

FIG. 8. The correspondence between classical dynamics and quantum entanglement entropy for the single-photon Dicke model with fixed particle number $N = 10$ and coupling constant $g = 0.5$. Parts (a)–(c) correspond to the classical phase spaces for the one-photon Dicke model with system energy $E = 1$, 4, and 7, respectively. Parts (d)–(f) denote the time-averaged entanglement entropy for the one-photon Dicke model with system energy $E = 1$, 4, and 7, respectively. Here we set $\omega = \omega_0 = 1$.

the classical phase spaces. The points A_1, A_3, B_2, B_3, C_2, and C_3 are in the classical chaotic region, but the points A_2, A_4, B_1, and C_1 are in the classical regular region. As the energy of the system $E = 1$, from Figs. 1(d) and 1(g) it seems that the linear entanglement entropy increases more rapidly for the initial states corresponding to these points in the classical chaotic region. However, the values of linear entanglement entropy for the points A_1–A_4 are so close that they sometimes overlap, which means that it is actually difficult to distinguish classical chaotic and regular behaviors by using the linear entanglement entropy in this case. With the increase of the energy of system E, one can obtain that the linear entanglement entropies of the points in the chaotic and regular regions become more distinguishable. As $E = 10$, from Figs. 1(f) and 1(i), we find that with time the linear entanglement entropy tends to different limit values for different initial states. The limit value of linear entanglement entropy for the states corresponding to the points (C_2, C_3) in the chaotic regions is much higher than that of the points (C_1) in the regular regions. This means that higher energy of a system can enhance the availability of entanglement entropy as a tool to explore quantum chaos in the two-photon Dicke model.

Now, we adopt the time-averaged entanglement entropy to investigate the correlation between classical dynamics and quantum entanglement in the two-photon Dicke model for different system energies. The time-averaged entanglement entropy is defined by

$$S_m = \frac{1}{T}\int_0^T S(t)dt, \tag{10}$$

where T is the total time of evolution. In Figs. 2(a)–2(c), we present the classical phase space for the two-photon Dicke model with system energy $E = 1$ for fixed coupling parameter $g = 0.1$, 0.25, and 0.4, respectively. The corresponding time-averaged entanglement entropy S_m with $T = 30$ is plotted in Figs. 2(d)–2(f) for the initial states related to the points in the whole classical phase space. In Fig. 2, comparing part (a) [or (c)] with part (d) [or (f)], it seems that there is a correspondence between the classical phase space and the distribution of time-averaged entanglement entropy, i.e., the initial state located in the chaotic region in classical phase space has high time-averaged entanglement entropy, and the initial state in the regular region has lower entanglement entropy. However, we also note that the time-averaged entanglement entropy for certain points that lie in the regular region is higher than that in the chaotic region. Actually, this behavior of time-averaged entanglement entropy in the few-particle regime is also found in the quantum kicked top model [39]. It is shown that in

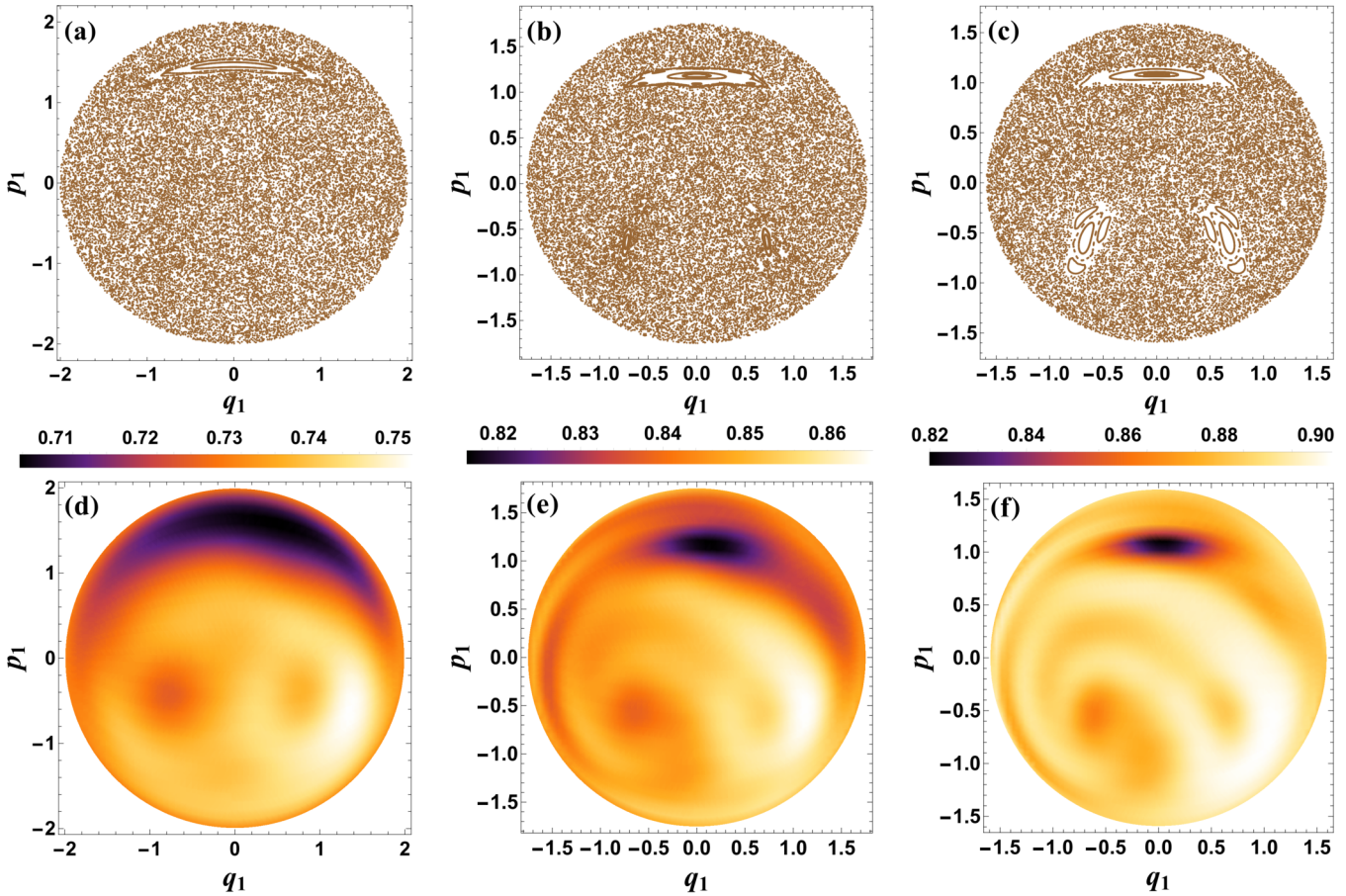

FIG. 9. The correspondence between classical dynamics and quantum entanglement entropy for the one-photon Dicke model with the fixed system energy $E = 4$ and coupling constant $g = 0.5$. Parts (a)–(c) correspond to the classical phase spaces for the single-photon Dicke model with particle number $N = 5$, 15, and 30, respectively. Parts (d)–(f) denote the time-averaged entanglement entropy for the one-photon Dicke model with particle number $N = 5$, 15, and 30, respectively. Here we set $\omega = \omega_0 = 1$.

the quantum kicked top system, the semiclassical limit is approached by increasing the particle number N, and then the correspondence between the classical phase space and the distribution of time-averaged entanglement entropy is improved. For the two-photon Dicke model, from Figs. 2(b) and 2(e), we can find directly that the corresponding relationship between the classical phase space and the time-averaged entanglement entropy does not hold in the few-particle case as the system energy is set to $E = 1$. In Fig. 3, we present the classical phase space and the time-averaged entanglement entropy for the two-photon Dicke model with the same parameters as in Fig. 2 except the system energy $E = 10$. Comparing Figs. 2 and 3, it is obvious that in the few-particle case ($N = 10$), higher system energy improves the correspondence between the classical phase space and the distribution of time-averaged entanglement entropy, which could be attributed to the fact that at high system energy a quantum state would expect thermalization to a "classical" high-temperature state.

It is well known that in the kicked top model, the structure of classical phase space does not depend on the number of particles N [11], thus it is convenient to compare the correlation between classical dynamics and quantum entanglement for systems with different N. However, in the two-photon Dicke model, one can find from Fig. 1 that the system energy affects the structure of the classical phase space. Actually, the structure of the classical phase space in the Dicke model does not change if the ratio E/N is fixed. In Fig. 4, we present the correspondence between classical dynamics and quantum entanglement for the two-photon Dicke model with a fixed ratio $E/N = 1.1$. We find that the correspondence is improved by increasing the energy E and the particle number N of the system at the same time. However, it is unclear which factor (the energy E or the particle number N) is responsible for this improvement. Thus, in order to probe the effects of the system energy E on the correspondence between classical dynamics and quantum entanglement entropy, as in the previous discussion, we have to change the system energy E and fix the particle number N in the two-photon Dicke model, although it will change the structure of the classical phase space. Actually, we can compare the degree of similarity between the classical Poincaré section and the distribution of quantum entanglement in the cases with different system energy and then probe further their correspondence. In Fig. 5, we present the correspondence between classical dynamics and quantum entanglement entropy for the two-photon Dicke model with a fixed particle number $N = 10$ and a coupling constant $g = 0.3$. It is obvious that the increase of E enhances the similarity between the classical Poincaré section and the distribution of

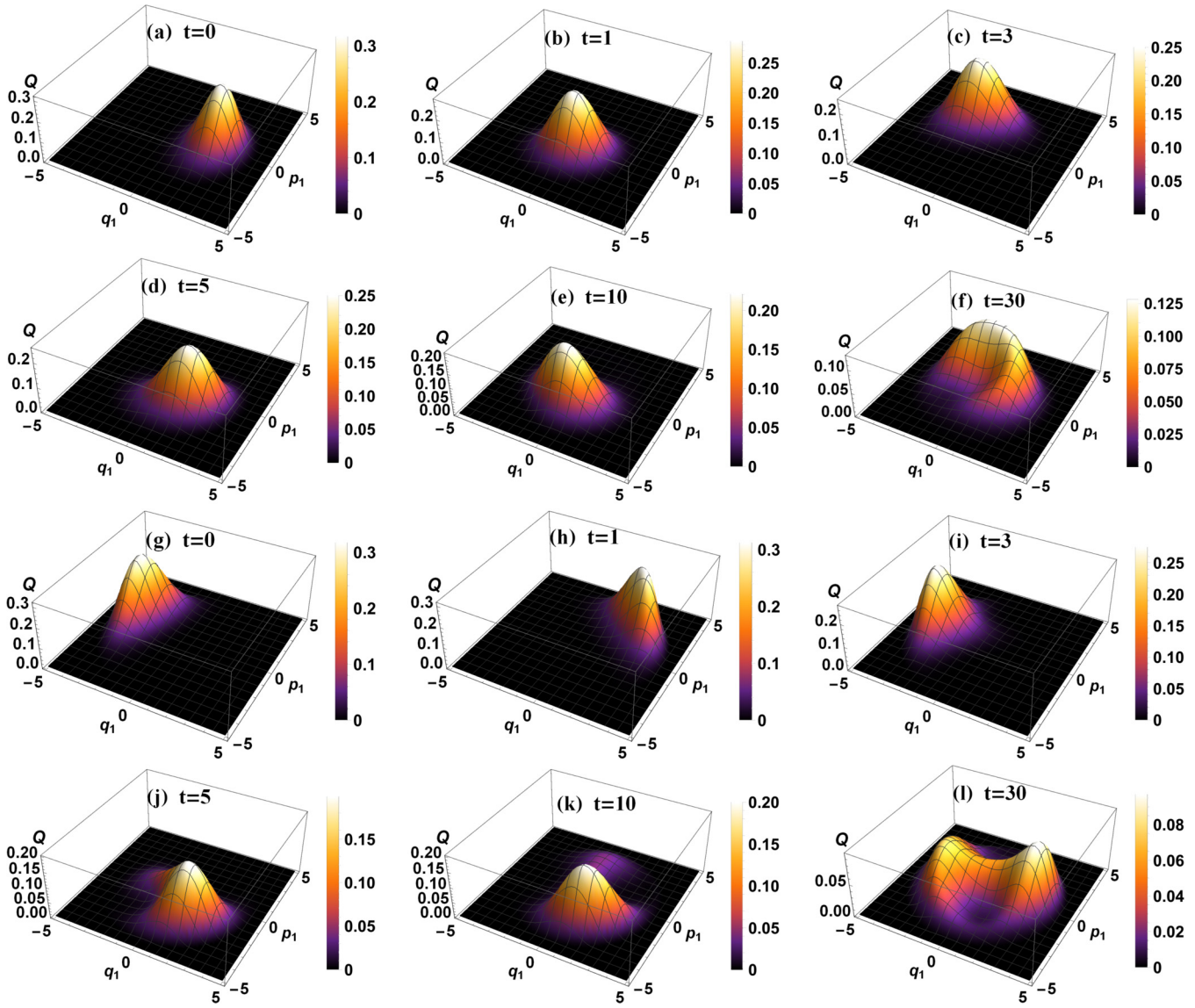

FIG. 10. Change of Husimi Q distribution with time for fixed coupling parameter $g = 0.3$ and system energy $E = 1$. Parts (a)–(f) denote the case in which the initial coherent state corresponds to point A_4 in the regular region in Fig. 1. Parts (g)–(l) denote the case in which the initial coherent state corresponds to point A_1 in the chaotic region in Fig. 1.

quantum entanglement entropy. Moreover, we find that with the increase of E, the time-averaged entanglement entropy for the initial state near the boundary in the classical phase space, which is in the chaotic region, becomes gradually higher than that for the initial state in the regular region. In Fig. 6, we find that the increase of the particle number N also improves the correspondence between classical dynamics and time-averaged entanglement entropy, which is similar to those obtained in the kicked top model [11]. To make a comparison, in Figs. 7–9, we plot the correspondence between classical dynamics and quantum entanglement entropy for the one-photon Dicke model. It is easy to find that the effects of the system energy E and the particle number N in the one-photon Dicke model are similar to those in the two-photon Dicke model. This also further supports the idea that an increase in the system energy E can improve the correspondence between classical dynamics and time-averaged entanglement entropy.

IV. HUSIMI Q DISTRIBUTION IN THE TWO-PHOTON DICKE MODEL

Husimi Q distribution is a quasiprobability distribution, which can provide a visualization of high-dimensional quantum states and demonstrates the dynamical evolution of the quantum state with time. It is shown that Husimi Q distribution displays a rapid dispersion over the phase space as the initial coherent state is in the classically chaotic region. Thus, with Husimi Q distribution, one can diagnose chaotic behavior in a quantum system [40]. For a coherent state, the Husimi Q function is defined as

$$Q(q_1, p_1) = \frac{1}{\pi}\langle q_1, p_1|\hat{\rho}_1|q_1, p_1\rangle, \tag{11}$$

where $|q_1, p_1\rangle$ is a coherent state and ρ_1 is the reduced-density matrix of the first subsystem. In Figs. 10 and 11, we present the change of Husimi Q distribution in phase

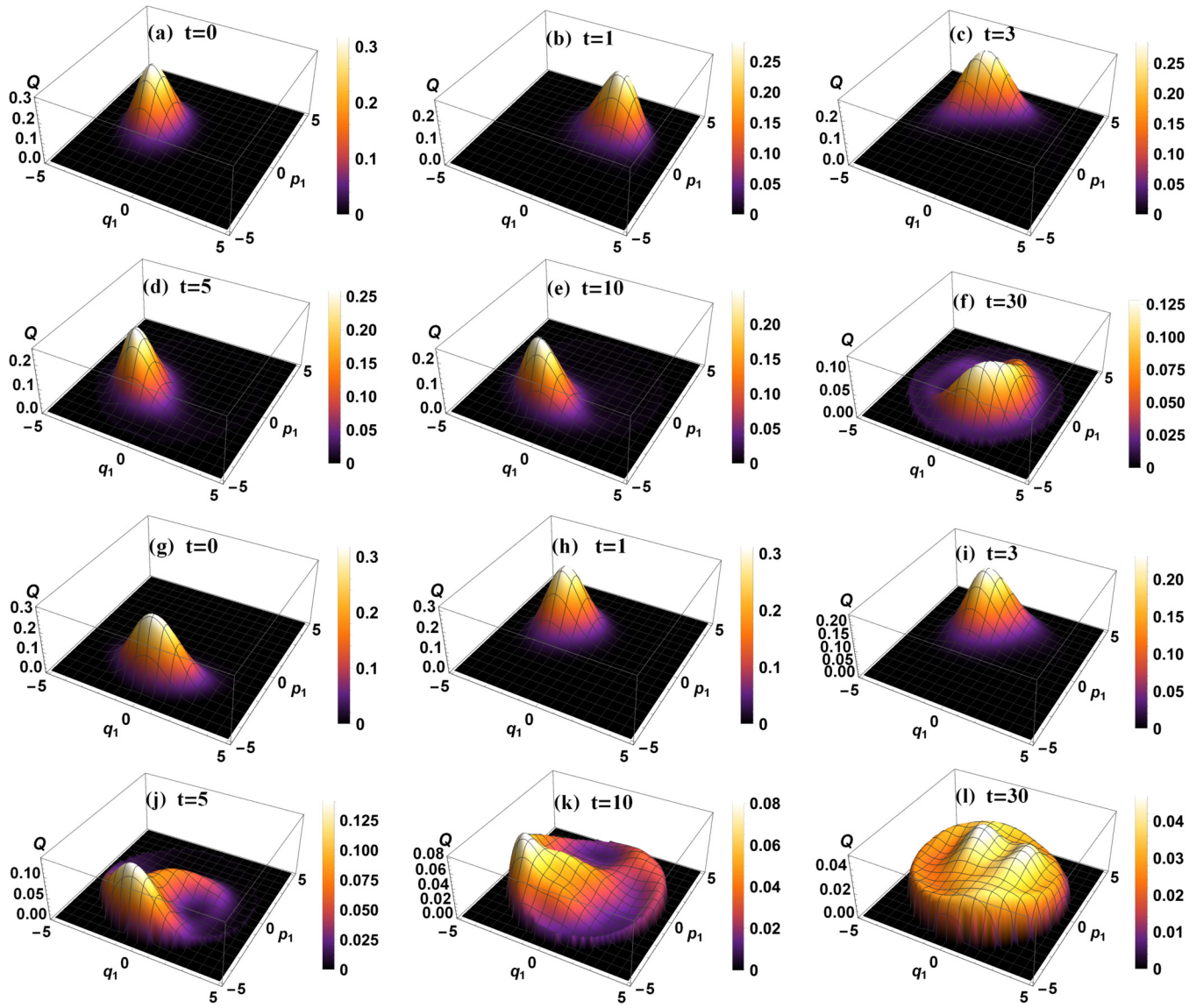

FIG. 11. Change of Husimi Q distribution with time for fixed coupling parameter $g = 0.3$ and system energy $E = 10$. Parts (a)–(f) denote the case in which the initial coherent state corresponds to point C_1 in the regular region in Fig. 1. Parts (g)–(l) denote the case in which the initial coherent state corresponds to point C_3 in the chaotic region in Fig. 1.

space for the quantum system with energy $E = 1$ and 10, respectively. Figures 10(a)–10(f) and 10(g)–10(l) demonstrate the dynamical evolution of the coherent state with the initial state corresponding to point A_4 in the regular region and point A_1 in the chaotic region in Fig. 1(a), respectively. The Husimi Q function has almost the same dispersion rate in the phase space for these two different states, which indicates again that it is difficult to distinguish classical chaotic and regular behaviors in the two-photon Dicke model with system energy $E = 1$. However, for the case with system energy $E = 10$, as shown in Fig. 11, one can find that the Husimi Q function for the initial state corresponding to point C_3 in the chaotic region disperses more quickly than that of the corresponding point C_1 in the regular region. Moreover, in Fig. 12 we present the variance of Husimi Q distribution for the quantum system with the same parameters as in Figs. 10 and 11. It shows that the variance of Husimi Q distribution for the initial state in the regular region decreases at almost the same rate in both cases $E = 1$ and 10. However, the variance in the chaotic region in the case $E = 10$ decays more quickly than that in the case $E = 1$. This means that the difference of the variance of Husimi Q distribution between in the chaotic and regular regions is more distinct in the case with higher system energy. Therefore, the change of Husimi Q distribution also supports the idea that higher system energy has contributed to distinguishing between chaotic and regular behavior in the quantum two-photon Dicke model.

Finally, we make a brief comparison of our results with other related studies. In the quantum kicked top model, it is found that the correspondence between the classical phase space and the distribution of time-averaged entanglement entropy can be improved by increasing the particle number N [11,15,39], which is totally understandable since as N (or j) tends toward infinite, the behavior of the quantum system indeed converges to that in the classic limit. In the one-photon and two-photon Dicke models, we find that the

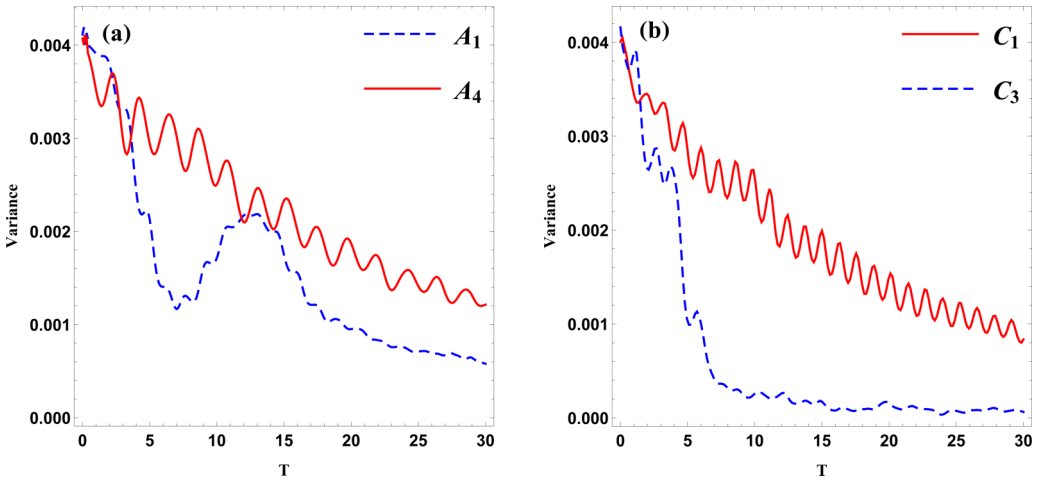

FIG. 12. Change of the variance in Husimi Q distribution with time for fixed coupling parameter $g = 0.3$ and $\omega = \omega_0/2 = 1$. In the left panel, the dashed blue and red lines correspond to the initial coherent states located at point A_4 in the regular region and point A_1 in the chaotic region, respectively, in Fig. 1(a) with the system $E = 1$. In the right panel, the dashed blue and red lines correspond to the initial coherent states located at point C_1 in the regular region and point C_3 in the chaotic region, respectively, in Fig. 1(c) with the system $E = 10$.

high system energy can improve the correspondence between classical phase space and the distribution of time-averaged entanglement entropy, which is not found elsewhere. This could be attributed to the fact that at high system energy, a quantum state would expect thermalization to a "classical" high-temperature state. Moreover, we also studied the effect of the particle number N in the Dicke model on the correspondence between chaos and entanglement entropy, and we found some similar results obtained in the quantum kicked top model. Therefore, our results indicate that the corresponding chaos and entanglement entropy can be improved by increasing both the particle number N and the system energy in the Dicke models.

V. SUMMARY

We have studied entanglement entropy and Husimi Q distribution in the two-photon Dicke model. It is shown that in the cases with higher system energy, the increasing rate of linear entanglement entropy becomes more rapid for the initial states corresponding to these points in the classical chaotic region. With the increase of the energy of the system, the values of linear entanglement entropy of the points in these chaotic and regular regions become more distinguishable. Moreover, there is an obvious improvement in the corresponding relationship between the distribution of time-averaged entanglement entropy and the classical Poincaré section in the cases with higher system energy. Finally, we also present Husimi Q distribution for a coherent state in the two-photon Dicke model with different system energies, and we find that Husimi Q distribution for the initial state corresponding to the point in the chaotic region in the higher-energy system disperses more quickly than that in the lower-energy system. This implies that higher system energy has contributed to distinguishing between the chaotic and regular behavior in the quantum two-photon Dicke model. Moreover, our results indicate that in the Dicke model, the correspondence between chaos and entanglement entropy can be improved by increasing both the particle number N and the system energy E. It would be of interest to study further whether there exists an inherent connection between these two different methods, and whether there are other quantities that might improve the corresponding chaos and entanglement entropy, which could help us to obtain a deeper understanding of the chaos in the quantum system.

ACKNOWLEDGMENTS

We would like to thank the anonymous referee for useful comments and suggestions. This work was partially supported by the National Natural Science Foundation of China under Grant No. 11875026, and the Scientific Research Fund of Hunan Provincial Education Department Grant No. 17A124. J.J.'s work was partially supported by the National Natural Science Foundation of China under Grant No. 11875025.

[1] G. Casati and B. Chirikov, *Quantum Chaos: Between Order and Disorder* (Cambridge University Press, Cambridge, UK, 1995).
[2] H. Stockmann, *Quantum Chaos: An Introduction* (Cambridge University Press, Cambridge, UK, 1999).
[3] F. Haake, *Quantum Signatures of Chaos* (Springer, Berlin, 2001).
[4] M. C. Gutzwiller, *Chaos in Classical and Quantum Mechanics* (Springer, New York, 1990).
[5] E. Wigner, Characteristic vectors of bordered matrices with infinite dimensions, Ann. Math. **62**, 548 (1955).
[6] F. J. Dyson, The threefold way. Algebraic structure of symmetry groups and ensembles in quantum mechanics, J. Math. Phys. **3**, 1199 (1962).

[7] K. Furuya, M. C. Nemes, and G. Q. Pellegrino, Quantum Dynamical Manifestation of Chaotic Behavior in the Process of Entanglement, Phys. Rev. Lett. **80**, 5524 (1998).

[8] X. W. Hou and B. Hu, Decoherence, entanglement, and chaos in the Dicke model, Phys. Rev. A **69**, 042110 (2004).

[9] G. Casati, I. Guarneri, and J. Reslen, Classical dynamics of quantum entanglement, Phys. Rev. E **85**, 036208 (2012).

[10] M. A. Valdez, G. Shchedrin, M. Heimsoth, C. E. Creffield, F. Sols, and L. D. Carr, Many-Body Quantum Chaos and Entanglement in a Quantum Ratchet, Phys. Rev. Lett. **120**, 234101 (2018).

[11] M. Lombardi and A. Matzkin, Entanglement and chaos in the kicked top, Phys. Rev. E **83**, 016207 (2011).

[12] A. Tanaka, Quantum mechanical entanglements with chaotic dynamics, J. Phys. A **29**, 5475 (1996).

[13] R. M. Angelo, K. Furuya, M. C. Nemes, and G. Q. Pellegrino, Rapid decoherence in integrable systems: A border effect, Phys. Rev. E **60**, 5407 (1999).

[14] J. B. Ruebeck, J. Lin, and A. K. Pattanayak, Entanglement and its relationship to classical dynamics, Phys. Rev. E **95**, 062222 (2017).

[15] A. Piga, M. Lewenstein, and J. Q. Quach, Quantum chaos and entanglement in ergodic and non-ergodic systems, Phys. Rev. E **99**, 032213 (2019).

[16] L. C. Evans, Towards a quantum analog of weak KAM theory, Commun. Math. Phys. **244**, 311 (2004).

[17] G. Hose, H. S. Taylor, and A. Tip, A quantum KAM-like theorem. ii. fundamentals of localisation in quantum theory for resonance states, J. Phys. A **17**, 1203 (1984).

[18] G. P. Brandino, J. S. Caux, and R. M. Konik, Glimmers of a Quantum KAM Theorem: Insights from Quantum Quenches in One-Dimensional Bose Gases, Phys. Rev. X **5**, 041043 (2015).

[19] T. Geisel, G. Radons, and J. Rubner, Kolmogorov-Arnol'd-Moser Barriers in the Quantum Dynamics of Chaotic Systems, Phys. Rev. Lett. **57**, 2883 (1986).

[20] L. J. Song, D. Yan, J. Ma, and X. G. Wang, Spin squeezing as an indicator of quantum chaos in the Dicke model, Phys. Rev. E **79**, 046220 (2009).

[21] V. Madhok, V. Gupta, D. A. Trottier, and S. Ghose, Signatures of chaos in the dynamics of quantum discord, Phys. Rev. E **91**, 032906 (2015).

[22] D. A. Roberts and D. Stanford, Diagnosing Chaos Using Four-Point Functions in Two-Dimensional Conformal Field Theory, Phys. Rev. Lett. **115**, 131603 (2015).

[23] E. B. Rozenbaum, S. Ganeshan, and V. Galitski, Lyapunov Exponent and Out-of-Time-Ordered Correlator's Growth Rate in a Chaotic System, Phys. Rev. Lett. **118**, 086801 (2017).

[24] I. García-Mata, M. Saraceno, R. A. Jalabert, A. J. Roncaglia, and D. A. Wisniacki, Chaos Signatures in the Short and Long Time Behavior of the Out-of-Time Ordered Correlator, Phys. Rev. Lett. **121**, 210601 (2018).

[25] S. Stufler, P. Machnikowski, P. Ester, M. Bichler, V. M. Axt, T. Kuhn, and A. Zrenner, Two-photon Rabi oscillations in a single $In_xGa_{1-x}As/GaAs$ quantum dot, Phys. Rev. B **73**, 125304 (2006).

[26] E. del Valle, S. Zippilli, F. P. Laussy, A. Gonzalez-Tudela, G. Morigi, and C. Tejedor, Two-photon lasing by a single quantum dot in a high-Q microcavity, Phys. Rev. B **81**, 035302 (2010).

[27] P. Bertet, S. Osnaghi, P. Milman, A. Auffeves, P. Maioli, M. Brune, J. M. Raimond, and S. Haroche, Generating and Probing a Two-Photon Fock State with a Single Atom in a Cavity, Phys. Rev. Lett. **88**, 143601 (2002).

[28] X.-F. Zhang, Q. Sun, Y.-C. Wen, W.-M. Liu, S. Eggert, and A.-C. Ji, Rydberg Polaritons in a Cavity: A Superradiant Solid, Phys. Rev. Lett. **110**, 090402 (2013).

[29] R. H. Dicke, Coherence in spontaneous radiation processes, Phys. Rev. **93**, 99 (1954).

[30] Q. H. Chen, C. Wang, S. He, T. Liu, and K. L. Wang, Exact solvability of the quantum Rabi model using Bogoliubov operators, Phys. Rev. A **86**, 023822 (2012).

[31] L. W. Duan, Y. F. Xie, D. Braak, and Q. H. Chen, Two-photon Rabi model: Analytic solutions and spectral collapse, J. Phys. A **49**, 464002 (2016).

[32] J. Peng, Z. Z. Ren, G. J. Guo, G. X. Ju, and X. Y. Guo, Exact solutions of the generalized two-photon and two-qubit Rabi, Eur. Phys. J. D **67**, 162 (2013).

[33] S. Felicetti, J. S. Pedernales, I. L. Egusquiza, G. Romero, L. Lamata, D. Braak, and E. Solano, Spectral collapse via two-phonon interactions in trapped ions, Phys. Rev. A **92**, 033817 (2015).

[34] L. Garbe, I. L. Egusquiza, E. Solano, C. Ciuti, T. Coudreau, P. Milman, and S. Felicetti, Superradiant phase transition in the ultrastrong-coupling regime of the two-photon Dicke model, Phys. Rev. A **95**, 053854 (2017).

[35] X. Y. Chen and Y. Y. Zhang, Finite-size scaling analysis in the two-photon Dicke model, Phys. Rev. A **97**, 053821 (2018).

[36] C. Emary and T. Brandes, Quantum Chaos Triggered by Precursors of a Quantum Phase Transition: The Dicke Model, Phys. Rev. Lett. **90**, 044101 (2003).

[37] C. Emary and T. Brandes, Chaos and the quantum phase transition in the Dicke model, Phys. Rev. E **67**, 066203 (2003).

[38] W. M. Zhang, D. H. Feng, and R. Gilmore, Coherent states: Theory and some applications, Rev. Mod. Phys. **62**, 867 (1990).

[39] M. Kumari and S. Ghose, Untangling entanglement and chaos, Phys. Rev. A **99**, 042311 (2019).

[40] S. Chaudhury, A. Smith, B. E. Anderson, S. Ghose, and P. S. Jessen, Quantum signatures of chaos in a kicked top, Nature (London) **461**, 768 (2009).